

Statistical analysis of comet disconnection events using STEREO HI and a data-assimilative solar wind model

Article

Accepted Version

Watson, S., Scott, C. ORCID: <https://orcid.org/0000-0001-6411-5649>, Owens, M. ORCID: <https://orcid.org/0000-0003-2061-2453>, Barnard, L. ORCID: <https://orcid.org/0000-0001-9876-4612> and Lang, M. (2025) Statistical analysis of comet disconnection events using STEREO HI and a data-assimilative solar wind model. *The Astrophysical Journal*, 982 (2). 66. ISSN 1538-4357 doi: [10.3847/1538-4357/adb978](https://doi.org/10.3847/1538-4357/adb978)
Available at <https://centaur.reading.ac.uk/121577/>

It is advisable to refer to the publisher's version if you intend to cite from the work. See [Guidance on citing](#).

To link to this article DOI: <http://dx.doi.org/10.3847/1538-4357/adb978>

Publisher: American Astronomical Society

All outputs in CentAUR are protected by Intellectual Property Rights law, including copyright law. Copyright and IPR is retained by the creators or other copyright holders. Terms and conditions for use of this material are defined in the [End User Agreement](#).


www.reading.ac.uk/centaur

CentAUR

Central Archive at the University of Reading

Reading's research outputs online

Statistical Analysis of Comet Disconnection Events Using STEREO HI and a Data-Assimilative Solar Wind Model

2 SARAH WATSON ¹, CHRIS SCOTT,¹ MATHEW OWENS,¹ LUKE BARNARD,¹ AND MATTHEW LANG²

3 ¹*University of Reading*

4 *Whiteknights House, Reading RG6 6UR*

5 ²*British Antarctic Survey*

6 *Cambridge, CB3 0ET*

7 ABSTRACT

8 Comets tails can reveal information about the local solar wind conditions. They can exhibit various
9 signatures of interactions with the solar wind including bending, developing kinks and sometimes a
10 undergoing tail disconnections. In this study, we investigate comet tail disconnection events observed in
11 the STEREO HI data during the period of 2007 to 2023. Using the Heliospheric Upwind eXtrapolation
12 model with a time-dependency (HUXt) solar wind model alongside novel solar wind data assimilation
13 (DA) techniques, each disconnection event was investigated to determine its cause. The resulting
14 statistical analysis led to three main conclusions; 1) For every Heliospheric Current Sheet (HCS)
15 crossing predicted by HUXt that occurs when the comet is within the region of influence of DA, a tail
16 disconnection follows, 2) For HCS crossings that occur outside the region where DA can be applied,
17 54.5% are followed by a tail disconnection, 3) There is an approximately linear relationship between
18 the speed of the solar wind at the HCS crossing and the time delay to the onset of a disconnection
19 given by the equation $V_{rel} \text{ (km s}^{-1}\text{)} = (2.23 \pm 0.35)\Delta t \text{ (hours)} + (400. \pm 10)\text{(km s}^{-1}\text{)}$.

20 1. INTRODUCTION

21 Comets are remnants from the early Solar System and they originate from the Oort cloud (Brownlee 2007). Some-
22 times a comet's orbit can take them into the inner Solar System and the icy rock subsequently sublimates into gas. This
23 process forms the coma, dust and plasma (ion) tails that we associate with comets (Götz et al. 2022). Comet tails are
24 affected by interactions with the solar wind and this is most prominent in their ion tails. **This study analyses solar
25 wind interactions with comet tails and therefore it focuses on the ion tail and not the dust tail.** The ion
26 tail can experience turbulence due to structures in the solar wind and this can be observed as bending or kinking of
27 the tail. The most dramatic evidence of solar wind interactions with the tail is a process called a disconnection event.
28 This is when the tail of the comet is removed from the nucleus. There are three widely accepted causes for discon-
29 nection events, all of which have been modelled or directly observed; The crossing of the heliospheric current sheet
30 (HCS) (Niedner & Brandt 1978), interaction with a stream interaction region (SIR) (Wegmann 2000) and the comet
31 encountering a coronal mass ejection (CME) (Vourlidas et al. 2008). Although individual case studies of comet-tail
32 disconnection events are valuable for explaining the types of solar wind conditions that can cause these events, it can
33 be difficult to determine if these mechanisms are common for all events or whether they were isolated incidents and
34 therefore comet dependent. In this study, 17 years of data taken from the Heliospheric Imagers (HIs) onboard the
35 NASA Solar TERrestrial RELations Observatory (STEREO) spacecraft (Kaiser et al. 2008) is used to analyse multiple
36 events to allow for a statistical investigation of comet-tail disconnections and to highlight any similarities between
37 them. Not only is this relevant to cometary science, but also for space weather forecasting and predictions, as comets
38 can be used to infer in-situ information about the solar wind, but this information is limited when the mechanism is
39 uncertain. The structure of this paper is as follows. In section 2, we discuss the influence of the heliospheric current
40 sheet as a cause for disconnection events. In section 3 we describe the methods used to carry out this analysis, which

are were previously tested on a singular case study. Section 4 shows the results obtained from the statistical study and finally in section 5, the results and their implications are summarised.

2. THE INFLUENCE OF THE HELIOSPHERIC CURRENT SHEET ON COMETS

The solar wind flows almost radially outwards from the Sun and drags the coronal magnetic field with it due to the frozen-in flux theorem (Alfvén 1942). Due to the rotation of the Sun, the magnetic field subsequently is wound into a spiral shape, known as the Parker spiral (Parker 1958). This extends into the Solar System. The heliospheric current sheet (HCS) is the boundary between the heliospheric magnetic field orientated towards and away from the Sun.

Alfvén proposed that the interplanetary magnetic field would get draped around a comet (Alfvén 1957) and form an induced magnetotail. It follows that any change in magnetic polarity that the comet experiences within the interplanetary magnetic field would have an effect on the comet. Niedner & Brandt (1978) explained what would happen if a comet experienced a change in polarity in the heliospheric magnetic field (also known as a crossing of the heliospheric current sheet) and showed that it would result in an ‘uprooting’ of the tail due to magnetic reconnection. This theory indicates that a comet should therefore always experience a tail disconnection when it encounters a magnetic field polarity change. There have been many studies on the impact of current sheet crossings on comets. For example, Brandt et al. (1999) found that no other property of the solar wind has a one-to-one association with disconnection events and this was supported by Voelzke & Matsuura (2000) who also found a clear association with disconnection events and ‘sector boundary’ (heliospheric current sheet) crossings. Yi et al. (1996) modelled the effects of a comet crossing the HCS, which resulted in a disconnection event. However, Voelzke (2005) summarised the theories and individual case studies on the association of disconnection events and current sheet crossings and it was found that although the relationship between them is accepted, it is less accepted that this association is one-to-one.

The uncertainty in the association between comets and HCS crossings could potentially be explained by a lack of accurate modelling of the heliospheric magnetic field out of the ecliptic plane, where in-situ information from spacecraft is extremely sparse, leading to the structure of the HCS at higher latitudes being less well understood. As comet orbits can be highly inclined, the lack of spacecraft data and observations at these latitudes could have resulted in less certainty when modelling the solar wind conditions at the comets. Comets are therefore a good probe in mapping the heliospheric magnetic field outside of the ecliptic plane. If we understand their association with the HCS, we can use techniques like Data Assimilation (DA) with observations of comets to improve modelling of the solar wind outside of the ecliptic.

3. METHOD

The core method used in this study is the same as the one used by Watson et al. (2024) in the individual case study of a tail disconnection observed by STEREO of Comet Leonard in December 2021. In that study, the method was developed to use assimilation of in-situ solar wind observations to constrain a solar wind model and hence determine the probable cause of a tail disconnection. In the current study, this method is applied to multiple events. Details of the method can be found in Watson et al. (2024), and are summarised in 3.2.

3.1. STEREO

The STEREO spacecraft (STEREO-A and STEREO-B) were launched in 2006, with the purpose of monitoring the Sun and inner heliosphere, to improve our understanding of space weather. Onboard both spacecraft is the Sun-Earth Connection Coronal and Heliospheric Investigation (SECCHI) instrument package (Howard et al. 2008), which contains the Heliospheric Imager-1 (HI-1) and Heliospheric Imager-2 (HI-2) instruments (Eyles et al. 2009). Early in the mission, these cameras provided a wide-field view of the Sun-Earth line. While these cameras were designed to image the solar wind and coronal mass ejections (CMEs), they have also captured other objects in their field of view such as comets. Due to their un-interrupted view, they are extremely useful for monitoring comet tails over extended periods of time. Such serendipitous observations of comets in the HI cameras were used for this study.

3.2. HUXt and Data Assimilation

The HUXt model (Owens et al. 2020; Barnard & Owens 2022) uses a reduced-physics approach to simulate the solar wind flow. It uses approximations to simplify the three dimensional magnetohydrodynamic (MHD) equations to one-dimensional incompressible hydrodynamics, greatly reducing model complexity and computation time. Despite the physical simplifications, it provides an output comparable to more sophisticated models (Riley & Lionello 2011) but at a fraction of the computational cost.

HUXt takes inner boundary conditions derived from coronal models such as the Wang-Sheeley-Argé (WSA) (Argé & Pizzo 2000), the Magnetohydrodynamics-About-A-Sphere (MAS) (Riley et al. 2001) or the Durham Magnetofrictional (DUMFRIC) (Yeates et al. 2010). These coronal models are all driven by remote observations of the photospheric magnetic field. They make estimates of the radial solar wind velocity and the radial magnetic field at 0.1 AU and these are used as the inner boundary conditions, which HUXt then propagates out into the inner solar system. For this study, the MAS coronal model is used with magnetograms from the Helioseismic and Magnetic Imager (HMI) onboard the Solar Dynamics Observatory (SDO) and the Michelson Doppler Imager (MDI) onboard the Solar and Heliospheric Observatory (SOHO). MAS simulates conditions throughout the corona and the conditions at $30R_{\odot}$ are extracted to be used as the boundary conditions for HUXt (plot a in figure 1). The solar wind speed is then subsequently determined and this solution is known as the prior state. Data for each Carrington rotation are available from <https://www.predsci.com/data/runs/>. Using this inner boundary input alone gives the prior state estimate of the solar wind at a given location in the solar system. However, this prior state can be improved by assimilating the in-situ data at Earth and the STEREO spacecraft. The reduced-physics approach of HUXt allows this technique to be used at a fraction of the computational cost of larger more complex MHD models.

Data assimilation (DA) is a method of combining observations with model output to produce a better estimate of reality. This has been applied to in-situ observations of the solar wind (Lang & Owens 2019) and has been used to improve solar wind forecasting in real-time (Turner et al. 2023). In a previous study by Watson et al. (2024), it was shown that assimilating the in-situ solar wind observations to improve boundary conditions for HUXt significantly improves the co-location of the comet with the heliospheric current sheet (HCS) - the likely cause of the subsequent tail disconnection event. The study demonstrated the value of using DA with the HUXt model for such comparisons. The same method is here applied to other comets captured in the STEREO field-of-view (FOV) to build up a statistical picture of comet-tail interactions.

In this study, the Burger Radial Variational Data Assimilation (BRaVDA) solar wind scheme was used (Lang & Owens 2019). The prior solar wind state is that provided by the MAS coronal model (plot a in figure 1). BRaVDA then assimilates the available spacecraft data for each day the comet is in the FOV. This was achieved by using the 27 day window centered on the day of calculation (Available spacecraft data consisted of STEREO-A, STEREO-B, and ACE. Note again that STEREO-B was out of operation after 2014 and therefore could not be used for comets that appeared after this) to produce updated inner boundary conditions, known as the 'posterior'. The full description of the BRaVDA methodology is found in Lang & Owens (2019). These posterior conditions are limited to the latitudes of available observations, i.e., the ecliptic plane and hence low heliographic latitudes. It is therefore necessary to combine the local-but-accurate information from posterior with the global-but-less-constrained information provided by MAS. This is achieved using a Gaussian filter, centered at the latitude of Earth with a latitudinal spread of $\pm 5^{\circ}$. **This number was chosen based on a study by Turner et al. (2021). It showed that the DA was more accurate when the observations were within 5 degrees separation of the Earth and the error that occurs from assuming the observations are on the ecliptic as opposed to their real location doesn't significantly impact the accuracy when the observations are within this 5 degrees.** Once the Gaussian filter has been applied, it produces a DA-updated MAS coronal map at 30 solar radii (plot b in figure 1) which is then input into HUXt as the updated boundary conditions. This technique only updates the solar wind speed, but the location of the HCS will also be improved as a result due to the propagation of these updated speeds.

As mentioned previously, when comparing modelled solar wind with comets, the comparison is expected to be most effective during the region where the comet is close to the ecliptic (i.e. at low heliographic latitudes). We refer to comets within $\pm 5^{\circ}$ as being 'within the region of influence of DA'. Estimates of the solar wind outside this latitude region are not necessarily unreliable, it is just that the data assimilation has less of an affect on the solar wind estimates and therefore the output is more representative of the model without data assimilation (the prior state). During this study, both comets within this region of $\pm 5^{\circ}$ of Earth and comets outside this region were investigated.

3.3. Disconnection Event Selection

The comet observations used in this study were selected from the monthly movies generated and made available by the HI Instrument team at <https://www.stereo.rl.ac.uk/cgi-bin/movies.pl>. This included data from STEREO A and STEREO B HI-1 and HI-2 cameras over the time period from December 2006 to December 2023 (contact was lost with STEREO B in 2014). From the movies in which there was a comet visible, not all contained a disconnection event. In addition, some movies contained a comet but the resolution of the instrument was not sufficient to be used

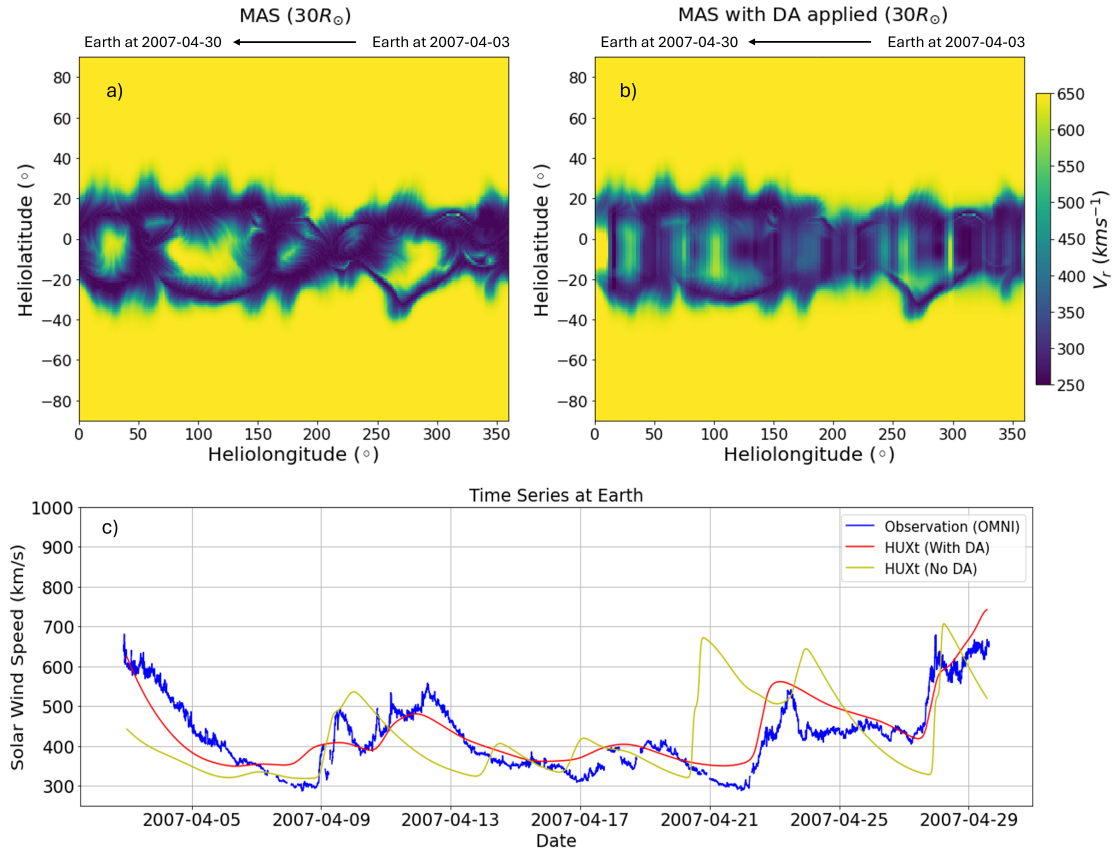


Figure 1. Visualisation of the methodology. Plot a) shows the Carrington longitude-heliolatitude map of solar wind speed at 30 solar radii from MAS. Plot b) shows the updated Carrington longitude-heliolatitude map of solar wind speed at 30 solar radii from MAS after data assimilation has been applied using a Gaussian filter, centered at the latitude of Earth with a latitudinal spread of $\pm 5^\circ$. Plot c) shows the subsequent time series at Earth, using these MAS solutions as inputs for HUXt. (**Note if the solar-wind structure is time stationary, this is a mirror image of the Carrington map. As well as this, there is a phase shift between the maps and the time series due to the solar wind taking a few days to reach Earth.**) The yellow line shows the MAS/HUXt model run (No Data-Assimilation) and the red line shows the MAS/BRAVDA/HUXt model run (Data-Assimilation). The observational data obtained from OMNI is shown in blue over the same time period.

141 for our analysis and so were eliminated from the study. See examples of these types of comets in figure 2. The left
 142 image is an example of when the comet tail became insufficiently visible over time and therefore some of the period
 143 it is in the FOV is used for analysis. The right image is an example of a comet which was eliminated from the study
 144 from the outset as the tail is hard to distinguish due to the presence of a CME which is also in the image. There were
 145 also comets which did not appear to have a visible tail during their time in STEREO FOV due to it appearing too
 146 faint in the images. Finally, some comets were eliminated due to the length of time they were in the FOV being too
 147 short for the type of analysis carried out in this study (less than one day). Following a detailed study of the HI data,
 148 over 30 comets were identified, but many were insufficient to analyse due to the criteria listed previously. Therefore,
 149 only 11 comets were selected for analysis which resulted in 13 separate appearances (comet 2P/Encke appeared three
 150 times over the 17 years of data). Of these 11 comets, 24 disconnection events were observed, see table 1. For the
 151 purpose of this study, a disconnection event was regarded as a disruption in the tail which resulted in a section of
 152 the tail becoming detached and observed to be carried away from the cometary nucleus, as observed from STEREO,
 153 see example in figure 3. For consistency, the start of an observed disconnection event was as the point at which the
 154 disruption first becomes visible. Three of the comets did not undergo any disconnection event during their period of
 155 time in STEREO, but these were still included in the analysis as a way to validate any findings.

4. RESULTS

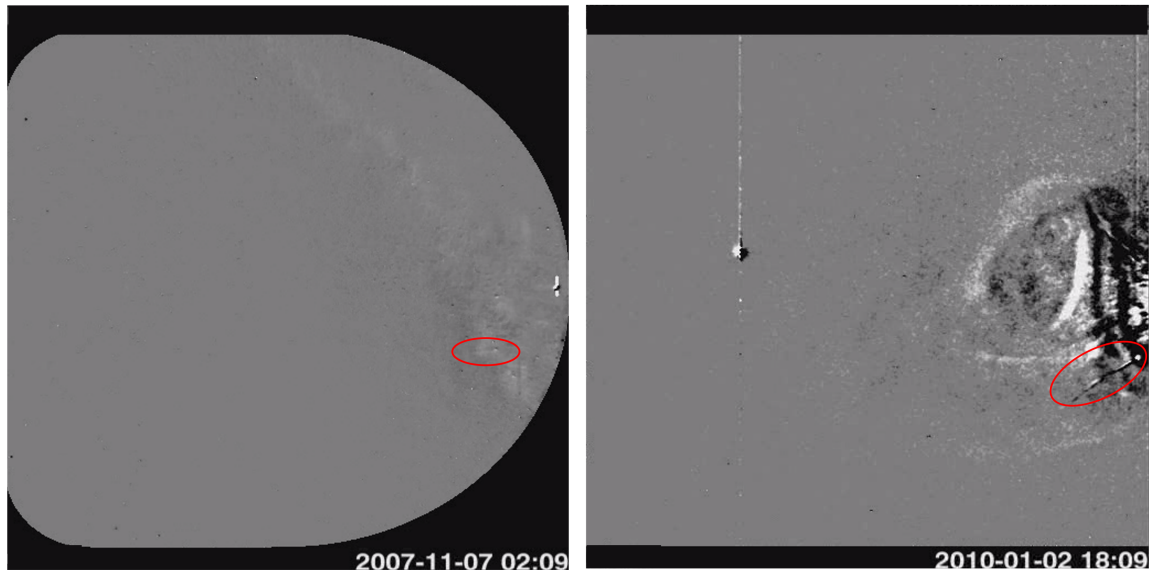


Figure 2. Some examples of periods where a comet is within the FOV of the STEREO HI camera but the tail is not sufficiently visible to determine if a disconnection event has occurred. The left image is of a comet (indicated by the red circle) where the tail is barely visible due to the viewing angle and therefore any disconnection event cannot be determined. This particular comet did have a period prior to this where the tail was sufficiently visible, so the comet was included in the study, but the period where the tail was non-resolvable is represented by the yellow shaded regions on the plots in the analysis. The right image is of a comet whose tail is un-resolvable due to the presence of a coronal mass ejection blocking the view. This is an example of a comet which was removed from the analysis.



Figure 3. An example of a 'disconnection event' that was used in this study. This is a series of three images from the STEREO HI-2 camera. The comet nucleus is circled in red for each image and the kink and disconnected tail which represent the disconnection event are also labeled. In the left image you can see the tail of the comet intact. The middle image shows the comet in the process of a tail disconnection, with a clear kink formed in the tail. The final image shows the end of the tail no longer attached to the main tail.

157 In total, 24 disconnection events were observed. Some comets experienced more disconnections than others. There
 158 did not appear to be any obvious reason for this. There was no apparent correlation with phase of the solar cycle
 159 nor a correlation between the heliospheric latitude/longitude of the disconnection and the frequency of occurrence.
 160 The three comets which did not appear to experience a disconnection all occurred when the Sun was in a period of
 161 solar minimum, however there were also other comets which did undergo a disconnection during solar minimum. The
 162 latitudinal extent of the HCS does vary with the solar cycle. At solar minimum, the HCS is located close ($\sim \pm 10^\circ$)
 163 to the solar equator, but at solar maximum it can extend to higher solar latitudes (reaching up to $\pm 90^\circ$) e.g figure
 164 5 in Owens (2020). This could suggest that during solar maximum, comets will experience HCS crossings at higher

Comet Name	STEREO Camera	Dates Visible (yyyy-mm-dd)	Disconnection Events	Distance from Sun of Disconnection (AU)
96P	HI-1A	2007-04-01 to 2007-04-07	None	-
2P (Encke)	HI-1A and HI-2A	2007-04-10 to 2007-04-29	2	0.34, 0.38
C/2007 F1	HI-1A and HI-2A	2007-10-27 to 2007-11-14	3	0.40, 0.42, 0.44
C/2011 W3	HI-1A and HI-2A	2011-12-12 to 2011-12-31	1	0.19
C/2011 L4	HI-1B and HI-2B	2013-03-10 to 2013-03-16	3	0.31, 0.32, 0.34
2P (Encke)	HI-1A and HI-2A	2013-11-14 to 2013-11-30	3	0.35, 0.34, 0.38
C/2012 S1	HI-1A and HI-2A	2013-11-21 to 2013-11-27	2	0.39, 0.30
C/2014 E2	HI-2A	2014-07-01 to 2014-07-23	2	0.66, 0.70
2P (Encke)	HI-1A	2017-03-01 to 2017-03-17	None	-
C/2019 Y4	HI-1A	2020-05-26 to 2020-06-06	None	-
C/2020 S3	HI-1A	2020-11-15 to 2020-12-07	2	0.53, 0.48
C/2021 A1	HI-2A	2021-12-07 to 2021-12-23	4	0.75, 0.73, 0.71, 0.67
C/2023 P1	HI-1A	2023-09-18 to 2023-10-03	2	0.30, 0.37

Table 1. Table showing the comets used in this study, along with the STEREO camera that was used for the observations. Comet Encke appeared more than once during the time span of the data used so appears multiple times in the table. It shows the dates the comet was visible in the HI cameras. Note that sometimes the comet can be in the FOV but the tail is not visible enough to determine whether a disconnection event occurs and therefore the analysis does not always cover the entire period when the comet is in the FOV. Column four shows the number of disconnection events observed for each comet and the final column is the heliocentric distance they occurred.

latitudes as well as in the ecliptic, potentially increasing the number of crossings altogether. However, a statistical study of the Wind spacecraft data found that there is no significant correlation between the number of times the spacecraft crossed the HCS and the time in the solar cycle (Liou & Wu 2021).

4.1. Heliospheric Current Sheet Crossings-Disconnection Events

The simulated magnetic field polarity of the solar wind at each comet was plotted for the time period the comet was visible in STEREO, see figure 4. HCS crossings occur where the magnetic field polarity changes sign. There is variability in the number of times a comet crosses the current sheet, with some comets (for example comet C/2020 S3) not experiencing a current sheet crossing at all during the time it is in the STEREO FOV. The period where the DA is most reliable ($\pm 5^\circ$ latitudinal separation between the comet and Earth) is highlighted in gray for each comet. Some comets do not come close enough to this latitudinal band to be within the region of influence of the DA and therefore the DA does not alter the model output. This was due to the inclination of the orbit of the individual comets, with some having more inclined orbits than others and therefore spending less time near the ecliptic. As mentioned previously, solar wind values that have not been adjusted through data assimilation do not necessarily result in the analysis being unreliable, but DA does not contribute to the model outside of this region. Each observed disconnection event is represented by the vertical dashed black line. The view of some comets was obstructed for a period of time (for example where the tail was not easily detected in front of the background stars) and there were time periods where no images were returned from the STEREO spacecraft. These are represented by the yellow shaded area on the plots. Such time periods have been ignored. In total, 10 of the current sheet crossings take place within the region of influence of the DA (the gray shaded area). Of these, there are two for which there is no or unreliable data (the yellow area) and are therefore discounted from the study. For all instances where the HUXt solar wind model shows the comet crossing the heliospheric current sheet within the gray shaded region, a disconnection event follows within 48 hours. There is a variety in the length of time after the crossing until the onset of the disconnection, this is explored in section 5.4.

To test the converse case, that there were no HCS crossings for those comets that did not undergo a disconnection event, the comets that experienced no disconnection event during their time in the STEREO field of view were also

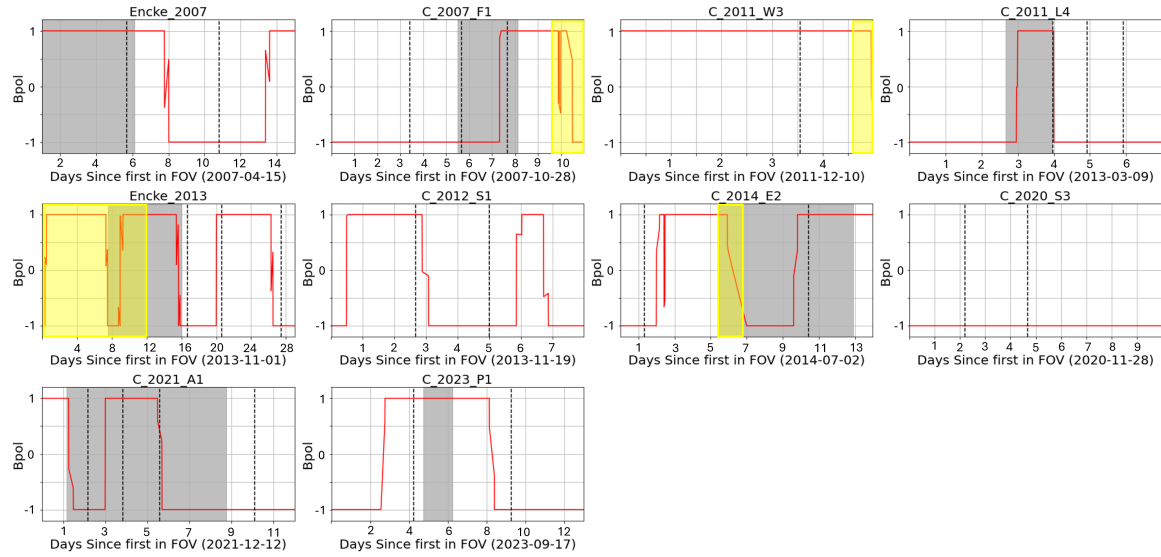


Figure 4. The nine comets (two are the same comet on its return) that were captured undergoing a disconnection event in the STEREO HI cameras. Each plot shows the simulated magnetic field polarity of the solar wind at the comet during its time in the STEREO field of view. The x-axis is labelled as number of days since the comet entered the FOV, which is also stated in brackets for each comet. The vertical black dashed lines show the time of the disconnection event in the tail. The gray shaded area is the time period where the data assimilation is expected to have the greatest influence on the modelled solar wind. Four of the plots have yellow shaded regions. This indicates a time period where the data from the STEREO camera was not available or a period where it is hard to determine if a disconnection took place, for example if the tail cannot be seen.

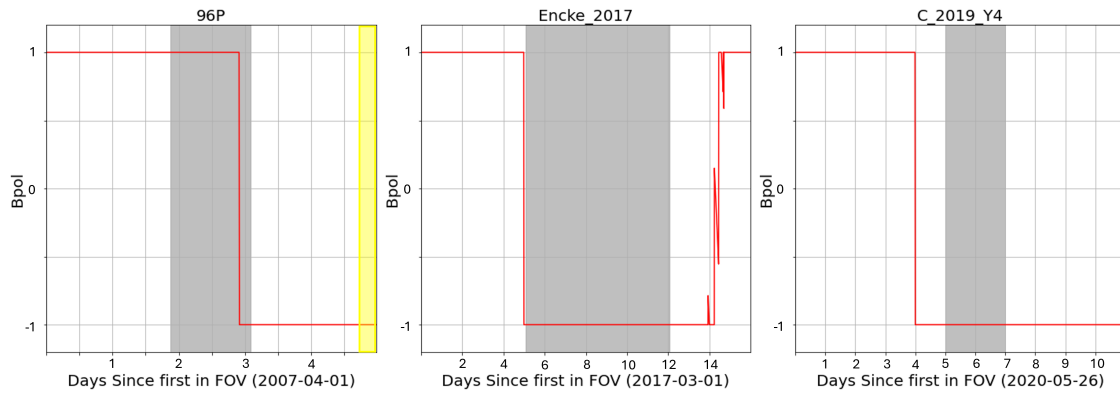


Figure 5. The three comets that were captured in the STEREO HI cameras but did not undergo a visible disconnection. Each plot shows the magnetic field polarity of the solar wind at the comet during its time in the STEREO field of view. The x-axis is labelled as number of days since the comet entered the FOV, which is also stated in brackets for each comet. The gray shaded area is the time period where the data assimilation of the model is most effective. The yellow shaded area indicates a time period where there is a data gap in the STEREO data or where it is hard to determine if a disconnection took place.

190 investigated. The results are show in figure 5. There were only three comets that did not undergo tail disconnection
 191 while in the field of view of the HI cameras; 96P, Encke/2P (2017) and C/2019 Y4. All three of these comets are
 192 observed during the region of influence of DA, shown by the gray shaded area. There was a period where the STEREO
 193 spacecraft had no data during the time Comet 96P was in the FOV and this is represented by the yellow shaded area,
 194 but there were no simulated HCS crossings in this region.

195 In summary, there was a total of 24 disconnection events observed and 25 current sheet crossings. Of the 25 current
 196 sheet crossings, 10 occurred within the region where the modeled solar wind was augmented by data assimilation and

15 occurred outside this region. Six crossings (2 in region of influence of DA, 4 outside the region of influence) were discounted as they occurred when there was no reliable data (yellow shaded area in figures). This left eight crossings which occurred at a latitude within the range of influence of DA, and 11 which occurred where DA did not contribute to the modeled solar wind values. In the discussion section, these are treated as separate categories for analysis. Finally, there were three comets which did not experience a disconnection event during their time in the STEREO FOV.

4.2. *The disconnection onset time delay as a function of solar wind speed*

A previous study by Niedner & Brandt (1979) suggested there should be a time delay between the magnetic field reversal (current sheet crossing) and the tail disconnection. The study suggested this to be approximately 18 hours, but this was based on one event (Niedner & Brandt 1979). This delay was also apparent in the results from this study and therefore this was investigated further. All events are shown on one figure (see figure 6), with the events that occur within the region of influence of DA shown in red and the events outside this region shown in black. Their respective regressions are shown individually (red and black dashed line) and the overall regression of all events is shown in blue. It should also be noted that for comet C/2011 L4, the first disconnection event is assumed to be as a result of the crossing of the previous current sheet and not the one which occurs at the same time, this is due to a disconnection not being an instantaneous event as the field lines take time to merge and begin the reconnection process (Niedner & Brandt 1979). Of the eight valid HCS crossings that occurred in the DA period, all were followed by a disconnection event. Of the 11 valid current sheet crossings that occurred outside of the region of influence of DA, six were followed by a disconnection event. **The radial speed of the comet was calculated using the ephemeris data and subtracted from the radial solar wind speed (provided by HUXt), giving the relative radial solar wind velocity at the comet, V_{rel} .** Note that the solar wind velocity can also be updated using DA and therefore the disconnections which occur within $\pm 5^\circ$ have a solar wind velocity which has been informed by in-situ observations at near Earth orbit. The time of the onset of the disconnection was determined using the STEREO imagery. The difference between this time and the time of the HCS crossing simulated by HUXt was then calculated and is given by Δt . The uncertainties in these methods have been taken into account and are shown in figure 6. The uncertainties result from the cadence of the HI images (40 minutes for HI-1 and 120 minutes for HI-2). Additionally, there is an uncertainty associated with the solar wind velocity at the HCS boundary simulated by the HUXt model. The solar wind velocity was taken as an average velocity over the time taken for the magnetic field to change polarity.

5. DISCUSSION

This statistical study has led to three main findings which are discussed in this section, but can be summarised as:

- For every HCS crossing predicted by HUXt when the comet is in the region of influence of DA, a comet tail disconnection follows
- For HCS crossings that occur in regions insensitive to the effects of DA, six out of 11 (54.5%) are followed by a comet tail disconnection
- Both the events for which DA can and cannot be applied show a broadly consistent correlation between the flow of the slow wind speed in the comets reference frame at the HCS crossing and the time delay to the onset of a disconnection

It should be noted that this study is not suggesting that every comet tail disconnection event is caused by crossing the HCS, only that for every crossing that the HUXt model identifies (within the region of influence of DA), a disconnection event follows. We are aware of other solar wind features that cause disconnection events, but HCS related disconnection events are the focus of this study.

5.1. *HCS Crossings when using the HUXt model informed by data assimilation*

When we isolated the HCS crossings that occurred within $\pm 5^\circ$ latitudinal separation from Earth, it was found that 100% of these crossings were followed by a disconnection event. We interpret this as evidence that DA-constrained HUXt simulations have some skill at predicting the interaction of the HCS with a comet, and that disconnection events are very likely to result from this interaction. From previous studies, mentioned in section 1, it has been suggested that comet-tail disconnections should always occur when a comet encounters the HCS. This study supports the theory that disconnection events do occur whenever a comet encounters the heliospheric current sheet for instances where DA

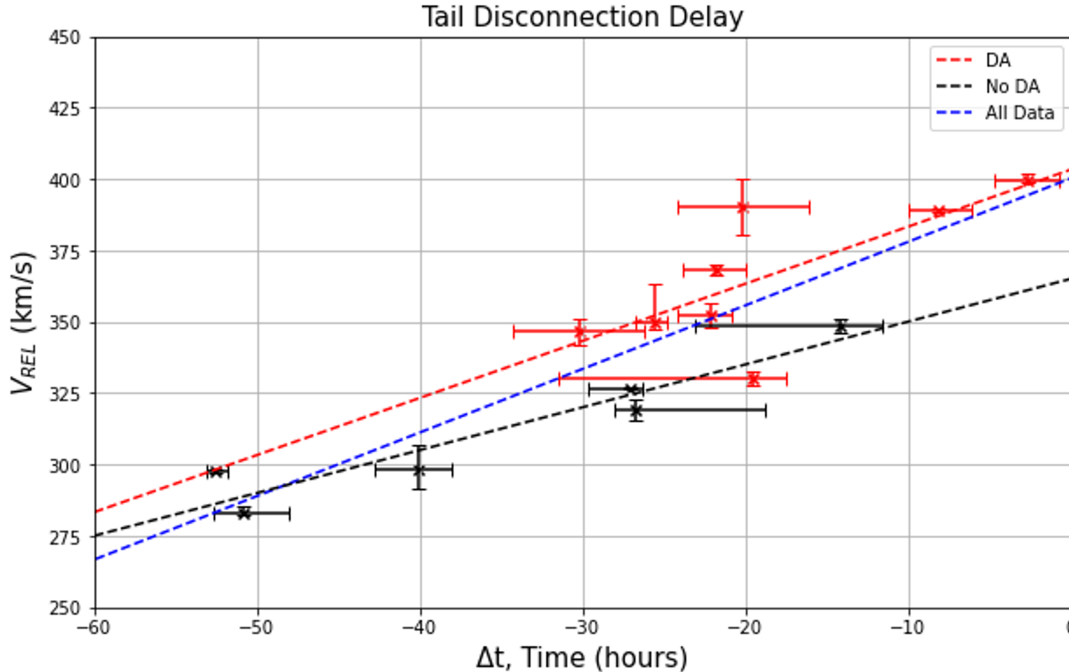


Figure 6. The comets that experienced a disconnection after a current sheet crossing are plotted. For each event, the delay time between crossing the current sheet and the onset of the disconnection was calculated and this was plotted against the radial solar wind speed at the time of the crossing. The comets which HUXt simulated crossing a current sheet when data assimilation could be used are shown in red. The corresponding regression line (red dashed line) is given by the equation $V_{rel} \text{ (km s}^{-1}\text{)} = (2.00 \pm 0.77) \Delta t \text{ (hours)} + (403 \pm 16) \text{ (km s}^{-1}\text{)}$. The comets which HUXt simulated crossing a current sheet when data assimilation could not be used are shown in black. The corresponding regression line (black dashed line) is given by the equation $V_{rel} \text{ (km s}^{-1}\text{)} = (1.5 \pm 0.24) \Delta t \text{ (hours)} + (365 \pm 9) \text{ (km s}^{-1}\text{)}$. The blue dashed line is the regression line of all events together, irrespective of if data assimilation could be applied or not and is given by the equation $V_{rel} \text{ (km s}^{-1}\text{)} = (2.23 \pm 0.35) \Delta t \text{ (hours)} + (400 \pm 10) \text{ (km s}^{-1}\text{)}$.

can enhance the HUXt solar wind model. This suggests that previous studies indicating that this relationship is not universal may have more to do with inaccuracies in the calculation of the position of the HCS in the solar wind model than the physical mechanism leading to comet tail disconnection. Furthermore, our result reinforces the conclusion that the use of DA in models such as HUXt is important for reproducing accurate solar wind conditions.

5.2. HCS Crossings when using HUXt model not informed by data assimilation

Comet orbits can be highly inclined to the ecliptic, meaning they cover a larger range of solar latitudes than Earth during their orbits. The technique of DA generates updated inner boundary conditions which then drive the HUXt model. It uses data from spacecraft (such as ACE and STEREO) which orbit close to the plane of Earth's orbit and also assumes that everything is in the ecliptic plane. As a result, the HUXt model outputs become less influenced by DA the further away from the latitude of Earth they are. In our study, there is a total of 15 HCS crossings which occur outside the region where DA influences the model. Of these, 11 crossings could be analysed in detail, of which 54.5% resulted in a tail disconnection. As an example, the second disconnection event experienced by comet Encke/2P (2007) occurred more than 70 hours after the HCS crossing predicted by the model which, taken in isolation would indicate that this was probably not the cause. Based on the conclusions from section 5.1, it is suggested that HUXt simulations of the HCS correlate one-to-one with tail disconnection events, however it should be considered that this is based on a small sample size of events and should be investigated further when more data is available. This one-to-one correlation does not occur where DA does not influence the HUXt solar wind estimates. Since there is evidence that DA improves the model, we conclude that the reduced correlation observed where DA does not influence the model could indicate model inaccuracies in the positioning of the current sheet beyond the ecliptic plane. This could be due to the coronal model/boundary condition inputs or due to the accuracy of the HUXt model itself. It should be noted

that HUXt is a 1D radial model and therefore there is no latitudinal evolution in the model. Any latitudinal structure shown is obtained from the boundary conditions and therefore as a result of the coronal model. This study highlights the need for improvements in modelling solar wind at higher latitudes as well as the importance of DA in solar wind models. It should be noted, we are not ruling out another cause to the reduction of disconnections following HCS crossings at high solar latitudes, although inaccuracies in the modelled latitudinal extent of the HCS could explain the discrepancy. This further supports the need to improve our understanding of the structure of the HCS outside of the ecliptic plane.

5.3. Comets with no disconnection events

Next, the comets where no disconnection event was observed were investigated. HUXt modelled no heliospheric current sheet crossings in gray shaded region and no disconnections followed. These results further support the reliability of HUXt when DA can be implemented and the one-to-one correlation of current sheet crossings and tail disconnections. Based on the HUXt model simulations of the HCS position, it is shown that Comets Encke/2P (2017) and C/2019 Y4 appear to cross the HCS during the time they are visible in STEREO, but these occur outside the region where the model was influenced by DA. Based on the results from section 5.2, we can assume that only 54.5% of comets undergo a tail disconnection when HUXt predicts a HCS crossing in this region where DA can be applied and that these two comets fell into the remaining 45.5% where the HCS has not been modelled using DA. Comet 96P is shown crossing the HCS during the optimum DA region, but no disconnection was observed. However, the STEREO HI cameras recorded no data for a period following the apparent crossing so while a disconnection could have occurred during this period, it was not possible to observe it. This is investigated further in section 5.5.

5.4. Velocity of Solar Wind against the Delay of the Disconnection

For each disconnection observed in STEREO, there appeared to be a time delay between the comet crossing the current sheet and the disconnection onset. The evidence of a time delay has been stated before by (Niedner & Brandt 1979). In our analysis, the time delay was calculated as the time at which HUXt modelled the comet crossing the current sheet to the time when the tail was first seen to undergo a disconnection. The disconnection events are shown in two categories, those that resulted from a current sheet crossing that occurred when the model was informed by DA (red), and those that occurred outside this region (black). This was to identify if there was a difference in trends between the two subsets which may result from differences in the accuracy of HUXt rather than the physical properties of the disconnection. Both show an increasing linear trend, with the larger the solar wind speeds associated with, more rapid onset of disconnections. This follows the theory proposed by (Niedner & Brandt 1979). They stated that the reconnection process of a comet when it enters a change in magnetic field polarity of the solar wind will first reconnect at the head of the comet, subsequently propagating down the tail, with the 'uprooting' of the tail being the final stage in the reconnection process. Assuming a similar IMF for all events (as the comets are imaged at a similar radial distance), the rate at which the field lines travel over the comet and reconnect must be related to the relative solar wind speed at the comet. The larger this speed, the greater the flux of magnetic field being draped over the comet nucleus leading to a quicker reconnection process. This would result in the detachment of the tail occurring sooner after the crossing of the current sheet.

This trend between the velocity and time delay has highlighted an important factor that should be considered if using comet tail disconnections as in-situ data points for space weather purposes. The non-instantaneous nature of a solar wind feature causing a disconnection event needs to be accounted for when using them to improve the positioning of certain features in solar wind models. This trend can also prove useful when identifying the solar wind speed at the comet and could provide a new technique of determining the local solar wind speed.

5.5. Investigating the 96P Anomaly

In section 5.3, it was mentioned that comet 96P was the only comet in the study that experienced a current sheet crossing during the DA period, but where no disconnection was observed. There was a period in which this comet was in the field of view of STEREO, but there was no data (HI camera did not take images). Therefore it would be of interest to test the relationship found in figure 6. As this crossing occurred in the region of influence of DA, it makes sense to use the relationship represented by the red dashed line in figure 6. This is as follows:

$$y = (2 \pm 0.77)x + (403 \pm 16)$$

where x is the time delay in hours and y is the solar wind speed in km s^{-1} at the time of the crossing. HUXt calculated the solar wind speed at the crossing to be approximately 317 km s^{-1} . From this, it would be expected that the time delay would be -43_{-40}^{+18} hours. Therefore the onset of the disconnection would be on 2007-04-05 18:51, and including errors could fall in range of 2007-04-05 01:13 to 2007-04-07 10:50. The STEREO spacecraft HI camera took its last image on 2007-04-05 at 18:50, and did not take another image until 2007-04-06 16:50. Therefore it cannot be ruled out that a disconnection did take place but that it occurred when there was no data.

6. CONCLUSIONS

Presented here is a statistical analysis of the comet-tail disconnection events observed in STEREO HI images over a period of 17 years of STEREO spacecraft operations. It was concluded that where DA influenced the output of the HUXt solar wind model, every heliospheric current sheet crossing was followed by a tail disconnection. Although this could be considered a small sample size, it does provide evidence of the accuracy of using DA with the HUXt model within the ecliptic. This one-to-one correlation of the model simulating a HCS crossing and a comet tail disconnection could lead to the use of comets in refining the position of the HCS. This would be particularly useful if the comet were in an L5 position as it could aid in improving the modelling of space weather heading towards Earth. When a comet crossed the heliospheric current sheet in regions where the model was not influenced by DA ($\pm 5^\circ$ latitudinal separation from Earth), only 54.5% of the crossings were followed by a disconnection. Based on the results from the crossings that occur when the model was informed by DA as well as the theory of comet tail disconnections, it was concluded that this difference was most likely down to reduced model performance at latitudes where there is more than $\pm 5^\circ$ latitudinal separation between the comet and Earth. We further conclude that improvements are needed in the modelling of the solar wind, particularly the position of the heliospheric current sheet, at latitudes outside the ecliptic. This study has also reiterated the importance of using DA in solar wind models to improve the correlation between the models and the observations.

By using observations from multiple comet-tail disconnection events, this study has also revealed a trend between the solar wind velocity and the time taken for the onset of a comet-tail disconnection after crossing the HCS. This trend not only supports the theory that the disconnection is not instantaneous, but also highlights the possibility of using this delay to determine the solar wind velocity at points in space beyond the reach of current spacecraft observations. The Polarimeter to UNify the Corona and Heliosphere (PUNCH) mission is set to launch in the near future (DeForest et al. 2022). This mission will provide higher spatial resolution and higher cadence HI images than STEREO. This will provide an opportunity to reduce the timing uncertainty on the comet-tail interaction, resulting in better constraints on the performance of DA within and outside the ecliptic.

This study has provided a novel statistical analysis of comet-tail disconnection events using the STEREO data and will have applications to those studying the physics of comet/solar wind interactions. Singular case studies of individual disconnection events are useful but can be contextual and they do not emphasise any important commonalities between events and therefore do not represent the more general properties of the solar wind and comet tail interactions. In addition, this study has application to the work of those studying the solar wind as it has highlighted potential differences between solar winds modelled within and outside the ecliptic plane. It also provides further evidence that using DA provides a means of improving solar wind models. Comets can be used to improve the modelling of the solar wind at more extreme latitudes and ultimately improve solar wind modelling for applications such as space weather forecasting.

7. ACKNOWLEDGMENTS

We thank the STEREO/HI instrument team at Rutherford Appleton Laboratory and the UK Solar System Data Centre for providing access to Heliospheric Imager data used. S. R. Watson is funded through STFC studentship ST/X508718/1. C. J. Scott and M. J. Owens are funded by STFC ST/V000497/1, M. J. Owens is also funded by NERC NE/Y001052/1. L. A. Barnard is funded by MR/Y021207/1.

8. DATA AVAILABILITY

The HUXt model used in this research can be downloaded at (<https://doi.org/10.5281/zenodo.6794462>) (Owens & Barnard 2022). HUXt version 4.0 was used in this work. BRaVDA can be accessed from (<https://doi.org/10.5281/zenodo.7892408>) (Lang 2023). The MAS inputs used were obtained from (<https://www.predsci.com/data/runs/>), using the MAS global coronal model to compute the solar wind at $30R_\odot$. Heliospheric Imager data was accessed from

361 UK Solar System Data Centre at (<http://www.ukssdc.rl.ac.uk/solar/stereo/data.html>). The STEREO HI data was
362 downloaded from RAL Space at (<https://www.stereo.rl.ac.uk/cgi-bin/movies.pl>).

REFERENCES

- 363 Alfvén, H. 1942, *Nature*, 150, 405, doi: [10.1038/150405d0](https://doi.org/10.1038/150405d0)
364 —. 1957, *Tellus*, 9, 92,
365 doi: [10.1111/j.2153-3490.1957.tb01855.x](https://doi.org/10.1111/j.2153-3490.1957.tb01855.x)
366 Arge, C. N., & Pizzo, V. J. 2000, *Journal of Geophysical*
367 *Research: Space Physics*, 105, 10465,
368 doi: <https://doi.org/10.1029/1999JA000262>
369 Barnard, L., & Owens, M. 2022, *Frontiers in Physics*, 10,
370 doi: [10.3389/FPHY.2022.1005621](https://doi.org/10.3389/FPHY.2022.1005621)
371 Brandt, J. C., Caputo, F. M., Hoeksema, J. T., et al. 1999,
372 *Icarus*, 137, 69, doi: [10.1006/icar.1998.6030](https://doi.org/10.1006/icar.1998.6030)
373 Brownlee, D. E. 2007, in *Treatise on Geochemistry*, ed.
374 H. D. Holland & K. K. Turekian (Oxford: Pergamon),
375 1–29,
376 doi: <https://doi.org/10.1016/B0-08-043751-6/01172-5>
377 DeForest, C., Killough, R., Gibson, S., et al. 2022, in 2022
378 IEEE Aerospace Conference (AERO), 1–11,
379 doi: [10.1109/AERO53065.2022.9843340](https://doi.org/10.1109/AERO53065.2022.9843340)
380 Eyles, C. J., Harrison, R. A., Davis, C. J., et al. 2009, *Solar*
381 *Physics*, 254, doi: [10.1007/s11207-008-9299-0](https://doi.org/10.1007/s11207-008-9299-0)
382 Götz, C., Deca, J., Mandt, K., & Volwerk, M. 2022.
383 <http://arxiv.org/abs/2211.04887>
384 Howard, R. A., Moses, J. D., Vourlidas, A., et al. 2008, *Br*,
385 136, 67, doi: [10.1007/s11214-008-9341-4](https://doi.org/10.1007/s11214-008-9341-4)
386 Kaiser, M. L., Kucera, T. A., Davila, J. M., et al. 2008,
387 *Space Science Reviews*, 136, 5,
388 doi: [10.1007/s11214-007-9277-0](https://doi.org/10.1007/s11214-007-9277-0)
389 Lang, M. 2023,
390 University-of-Reading-Space-Science/BRaVDA:
391 BRaVDA v1.9, Zenodo, doi: [10.5281/zenodo.7892408](https://doi.org/10.5281/zenodo.7892408)
392 Lang, M., & Owens, M. J. 2019, *Space Weather*, 17, 59,
393 doi: [10.1029/2018SW001857](https://doi.org/10.1029/2018SW001857)
394 Liou, K., & Wu, C.-C. 2021, *The Astrophysical Journal*,
395 920, 39, doi: [10.3847/1538-4357/ac1586](https://doi.org/10.3847/1538-4357/ac1586)
396 Niedner, Jr., M. B., & Brandt, J. C. 1978, *The*
397 *Astrophysical Journal*, 223, 655, doi: [10.1086/156299](https://doi.org/10.1086/156299)
398 —. 1979, *The Astrophysical Journal*, 234, 723,
399 doi: [10.1086/157549](https://doi.org/10.1086/157549)
400 Owens, M., & Barnard, L. 2022,
401 University-of-Reading-Space-Science/HUXt: HUXt 4.0,
402 Zenodo, doi: [10.5281/zenodo.6794462](https://doi.org/10.5281/zenodo.6794462)
403 Owens, M., Lang, M., Barnard, L., et al. 2020, *Solar*
404 *Physics*, 295, doi: [10.1007/s11207-020-01605-3](https://doi.org/10.1007/s11207-020-01605-3)
405 Owens, M. J. 2020, *Solar-Wind Structure*, Oxford
406 University Press,
407 doi: [10.1093/acrefore/9780190871994.013.19](https://doi.org/10.1093/acrefore/9780190871994.013.19)
408 Parker, E. N. 1958, *The Astrophysical Journal*, 128, 664,
409 doi: [10.1086/146579](https://doi.org/10.1086/146579)
410 Riley, P., Linker, J. A., & Mikić, Z. 2001, *Journal of*
411 *Geophysical Research: Space Physics*, 106, 15889,
412 doi: <https://doi.org/10.1029/2000JA000121>
413 Riley, P., & Lionello, R. 2011, *Solar Physics*, 270, 575,
414 doi: [10.1007/s11207-011-9766-x](https://doi.org/10.1007/s11207-011-9766-x)
415 Turner, H., Lang, M., Owens, M., et al. 2023, *Space*
416 *Weather*, 21, doi: [10.1029/2023SW003457](https://doi.org/10.1029/2023SW003457)
417 Turner, H., Owens, M. J., Lang, M. S., & Gonzi, S. 2021,
418 *Space Weather*, 19, e2021SW002802,
419 doi: [10.1029/2021SW002802](https://doi.org/10.1029/2021SW002802)
420 Voelzke, M. R. 2005, *Earth, Moon, and Planets*,
421 doi: [10.1007/s11038-006-9073-y](https://doi.org/10.1007/s11038-006-9073-y)
422 Voelzke, M. R., & Matsuura, O. T. 2000, *Astronomy and*
423 *Astrophysics Supplement Series*, 146,
424 doi: [10.1051/aas:2000259](https://doi.org/10.1051/aas:2000259)
425 Vourlidas, A., Davis, C., Eyles, C., et al. 2008, *The*
426 *Astrophysical Journal Letters*, 668, L79,
427 doi: [10.1086/522587](https://doi.org/10.1086/522587)
428 Watson, S. R., Scott, C. J., Owens, M. J., & Barnard, L. A.
429 2024, *The Astrophysical Journal*, 970, 101,
430 doi: [10.3847/1538-4357/ad50cf](https://doi.org/10.3847/1538-4357/ad50cf)
431 Wegmann, R. 2000, *Astron. Astrophys*, 358, 759
432 Yeates, A. R., Mackay, D. H., van Ballegooijen, A. A., &
433 Constable, J. A. 2010, *Journal of Geophysical Research:*
434 *Space Physics*, 115,
435 doi: <https://doi.org/10.1029/2010JA015611>
436 Yi, Y., Walker, R. J., Ogino, T., & Brandt, J. C. 1996,
437 *Journal of Geophysical Research: Space Physics*, 101,
438 27585, doi: [10.1029/96JA02235](https://doi.org/10.1029/96JA02235)